

3D Time Dependent Stokes Vector Radiative Transfer in an Atmosphere-Ocean System Including a Stochastic Interface

George W. Kattawar
Dept. of Physics
Texas A&M University
College Station, TX 77843-4242
phone: (409) 845-1180 fax: (409) 845-2590 email: kattawar@tamu.edu

Award Number: N000140610069
<http://people.physics.tamu.edu/trouble/work.html>

LONG-TERM GOALS

The major objective of this proposal is to calculate the 3-D, time dependent radiation field both within the ocean and in the atmosphere in the presence of a stochastically varying interface which may also be perturbed by sea foam, air bubbles, surfactants, rain, etc. This study will serve as the genesis to the future evolution of an inversion algorithm whereby one could reconstruct images that have been distorted by the interface between the atmosphere and the ocean or the ocean itself. This study will rely heavily on both the spectral and polarimetric properties of the radiation field to deduce both the sea state and the perturbations produced on it. A second phase of this study will be to explore the asymptotic polarized light field and to determine how much information can be obtained about the IOP's of the medium by measuring it. The third phase of this proposal will deal with the problem of improving image resolution in the ocean using some novel polarimetric techniques that we are just beginning to explore. Once these studies have been completed using a passive source, it will be rather straightforward to extend them to active sources where we can explore the use of both photo-acoustic and ultrasound-modulated optical tomography to improve image resolution.

OBJECTIVES

The new Navy initiative is focusing on one of the most formidable problems in radiative transfer theory; namely, calculating the full 3D time dependent radiation field (with full Mueller matrix treatment) in a coupled atmosphere-ocean system where the boundary separating the two has both spatial and temporal dependence. Although a great deal of work has been done on obtaining power spectra for ocean waves, I know of no work that has yielded similar results for the radiation field within the ocean. It is clear that as long as the surface has a significant effect on the internal light field, it will leave its signature on the radiation field within the ocean and the relative strength of this field compared to the ambient field will determine the success or failure of inversion algorithms. However, as we go deeper within the ocean we start to enter a region called the asymptotic region where all photons lose memory of their origin and the light field then remains stationary and becomes independent of the azimuthal angle. The depth dependence becomes simply exponential, i.e. $\mathbf{L}(z+h, \theta) = \mathbf{L}(z, \theta) \exp(-kh)$ where k is called the diffusion exponent. It should be noted at this juncture that this asymptotic light field is still polarized which is why we used the bold-faced vector notation. We were the first to compute the degree of polarization for this asymptotic light field for Rayleigh scattering and were able to obtain an analytic expression for both the polarized radiation field and the diffusion exponent (see ref. 1). In addition, we were also able to set up a numerical scheme to compute the polarized radiation field as well as the diffusion exponent for any single scattering Mueller matrix.

Report Documentation Page				Form Approved OMB No. 0704-0188	
Public reporting burden for the collection of information is estimated to average 1 hour per response, including the time for reviewing instructions, searching existing data sources, gathering and maintaining the data needed, and completing and reviewing the collection of information. Send comments regarding this burden estimate or any other aspect of this collection of information, including suggestions for reducing this burden, to Washington Headquarters Services, Directorate for Information Operations and Reports, 1215 Jefferson Davis Highway, Suite 1204, Arlington VA 22202-4302. Respondents should be aware that notwithstanding any other provision of law, no person shall be subject to a penalty for failing to comply with a collection of information if it does not display a currently valid OMB control number.					
1. REPORT DATE 30 SEP 2007		2. REPORT TYPE		3. DATES COVERED 00-00-2007 to 00-00-2007	
4. TITLE AND SUBTITLE 3D Time Dependent Stokes Vector Radiative Transfer In An Atmosphere-Ocean System Including A Stochastic Interface				5a. CONTRACT NUMBER	
				5b. GRANT NUMBER	
				5c. PROGRAM ELEMENT NUMBER	
6. AUTHOR(S)				5d. PROJECT NUMBER	
				5e. TASK NUMBER	
				5f. WORK UNIT NUMBER	
7. PERFORMING ORGANIZATION NAME(S) AND ADDRESS(ES) Texas A&M University, Dept. of Physics, College Station, TX, 77843				8. PERFORMING ORGANIZATION REPORT NUMBER	
9. SPONSORING/MONITORING AGENCY NAME(S) AND ADDRESS(ES)				10. SPONSOR/MONITOR'S ACRONYM(S)	
				11. SPONSOR/MONITOR'S REPORT NUMBER(S)	
12. DISTRIBUTION/AVAILABILITY STATEMENT Approved for public release; distribution unlimited					
13. SUPPLEMENTARY NOTES code 1 only					
14. ABSTRACT					
15. SUBJECT TERMS					
16. SECURITY CLASSIFICATION OF:			17. LIMITATION OF ABSTRACT Same as Report (SAR)	18. NUMBER OF PAGES 11	19a. NAME OF RESPONSIBLE PERSON
a. REPORT unclassified	b. ABSTRACT unclassified	c. THIS PAGE unclassified			

The interesting feature about the asymptotic light field is that it depends profoundly on both the single scattering albedo as well as the phase function of the medium. We also found that substantial errors will occur in both the ordinary radiance and the diffusion exponent if they are calculated from scalar rather than vector theory

APPROACH

There are several stages to our approach that we will enumerate. The sine qua non for this entire project will be the development of a fully time dependent 3-D code capable of calculating the complete radiation field, i.e. the complete Mueller or Green matrix at any point within the atmosphere-ocean system. This of course implies that both horizontal as well as vertical IOP's must be accounted for. It should also be noted that the code must be capable of handling internal sources as well in order to explore both fluorescence and bioluminescence. At present there are several 3D codes that are able to compute various radiometric quantities in inhomogeneous media; however, as far as we know, none exists which will couple both atmosphere and ocean with a time dependent stochastic interface. One of the earliest 3D radiative transfer (RT) codes was developed by Stenholm, et. al² to model thermal emission from spherical and non-spherical dust clouds. It was based on an implicit discretization of the transfer equation in Cartesian frames. To our knowledge, the first 3D-scalar RT code using discrete ordinates was written by Sánchez³ et al.; however, it did not make use of spherical harmonics and lacked efficiency and accuracy particularly for small viewing angles. The addition of polarization to the 3D discrete ordinates method was done by Haferman⁴ et al. Almost concurrently, a 3D-scalar RT code was written by K. F. Evans⁵ which used both spherical harmonics and discrete ordinates. This method uses a spherical harmonic angular representation to reduce memory and CPU time in computing the source function and then the RT equation is integrated along discrete ordinates through a spatial grid to model the radiation streams. We have already obtained this code and will use it for validation of our 3D scalar Monte Carlo code for both the atmosphere and ocean components. Several Monte Carlo codes both scalar and vector have been published for solving specialized problems in atmospheric optics usually dealing with finite clouds^{6,7,8,9}. Without exception, these codes are using quite primitive, also called "brute force", methods. None of them will do what we are proposing in our approach to the fully time dependent 3D solution applicable to both atmosphere and ocean. It should be mentioned that we have already successfully added to our Green matrix Monte Carlo code the capability to handle internal sources such as fluorescence, bioluminescence and even thermal emission.

Once we have developed our 3D code to handle both the ocean and atmosphere without the interface included, we will then develop a 3D form of 1D matrix operator theory that we worked out in two seminal papers published in Applied Optics^{10,11}. The basic idea of the method is that if one knows the reflection and transmission operators of say two layers, then it is rather straightforward to get the reflection and transmission operators for the combined layer. With this method we can start from an infinitesimal layer and build large and even semi-infinite layers in a rapid way, i.e. if we start with a layer of thickness Δ then in N steps we can reach a thickness of $2^N \Delta$. Another very relevant feature of this method is that it will allow us to add the interface to the "bare" ocean, i.e., one without an interface, to get the combined ocean-interface operator and then add this layer to the atmosphere for the final reflection and transmission operators for the combined system. The question immediately arises is why not solve the entire system at the same time? The answer is that by doing it this way we only have to use the adding feature to combine the time dependent interface thus avoiding performing the entire calculation at each instant in time. This method has also become known as the adding-doubling method. These operators are effectively the impulse response or Green matrix for the upper

and lower boundaries of the medium. Therefore, if we know the external radiance input into both upper and lower layers, we can then obtain the output at both the upper and lower boundaries of the combined system. A pictorial description of the method is shown in Fig. 1. It should be emphasized that this method will also handle internal sources as well such as bioluminescence, fluorescence, and even thermal emission. This method can also handle detectors at any interior point in the medium. Another bonus of matrix operator theory is that one can easily obtain the path radiance between source and detector which is a sine qua non for image analysis.

In order to add a interface which is spatially inhomogeneous in the y direction but homogeneous in the x direction, we will need the reflection (R) and transmission (T) operators for both the atmosphere and ocean now as a function of time t and both z and y ; namely $R(y-y_0, z, t, \theta, \phi)$ and similarly for T . It is important to note that we only have to obtain the response of the atmosphere or ocean to a single line source at the point y_0 and then using the translational invariance of the medium in the y -direction will have the reflection and transmission operators at every point in the y -direction. The only method we know to create these 2-D operators is Monte Carlo. Once these are obtained, we can use the output from each layer as the input to the surface boundary whose reflection and transmission properties are either known or calculable. For instance if the surface consists of just capillary or gravity waves, then we just need the Fresnel coefficients to give us the requisite reflection and transmission operators for the interface. Now once these operators are obtained then we can use extended matrix operator theory to get the final time dependent radiation field that a detector will see. Let us consider the simplest case where the surface is 1-D and we know its power spectrum. It should be emphasized at this point that it is not sufficient to have just a wave-slope distribution since it will only give us statistically averaged results for the radiance field. The introduction of the spatial and temporal dependent interface destroys the symmetry and makes all 1-D codes essentially useless in this domain. At each instant in time, the surface will have a distinct shape that will evolve in time. We have developed a method using linear filter theory whereby we can take an ocean power spectrum and using a random number generator create a realistic surface that will match the original power spectrum and will still exhibit both stationarity and ergodicity. Now the nice feature about what we are proposing is that we can now concentrate on just the effects of the surface on the detectors since as the surface evolves in time so too will the radiance field as recorded by the detectors. Now both the spatial and temporal profiles will be constantly changing; however, we will have created them from a medium which has been assumed stationary and only the interface produces the time dependence and the horizontal spatial inhomogeneities, i.e. the R and T operators for both the atmosphere and ocean need only to be computed **once**. This is clearly a first-order solution to the more complex problem; however, it should tell us a great deal about future complexities of inversion and also the efficacy of pursuing the next level of difficulty. If the surface is perturbed by foam, bubbles, etc. then these can be added and the matrix operator theory will be used to calculate the effective reflection and transmission operators of the perturbed surface. It should also be stated that this project is enormously computationally intensive; however, the type of codes we will produce are ideally suited for large-scale parallel processors, which we do have access to.

The next level of difficulty is where we will use Monte Carlo methods to compute a full 3-D distribution of the time dependent radiation field, which now may include 3-D inhomogeneities in both the ocean and atmosphere. This will be a computational tour de force requiring a major new computer program that must be capable of placing IOP's of both the atmosphere and ocean at each point in a large 3-D grid. Matrix operator theory will again be used but it will now be much more complicated since our reflection and transmission operators now become functions of three spatial variables. In fact, the complete solution to this problem could approach the complexity of the general circulation

models used in weather forecasting. Due to the large volume of data that will be generated, we will clearly have to develop methods to easily display animated sequences of this time dependence.

These projects are being worked on by Dr. Pengwang Zhai, a postdoctoral research associate, and Ms. Julie Slanker, who will complete her M.S. degree in Physics in December of 2007.

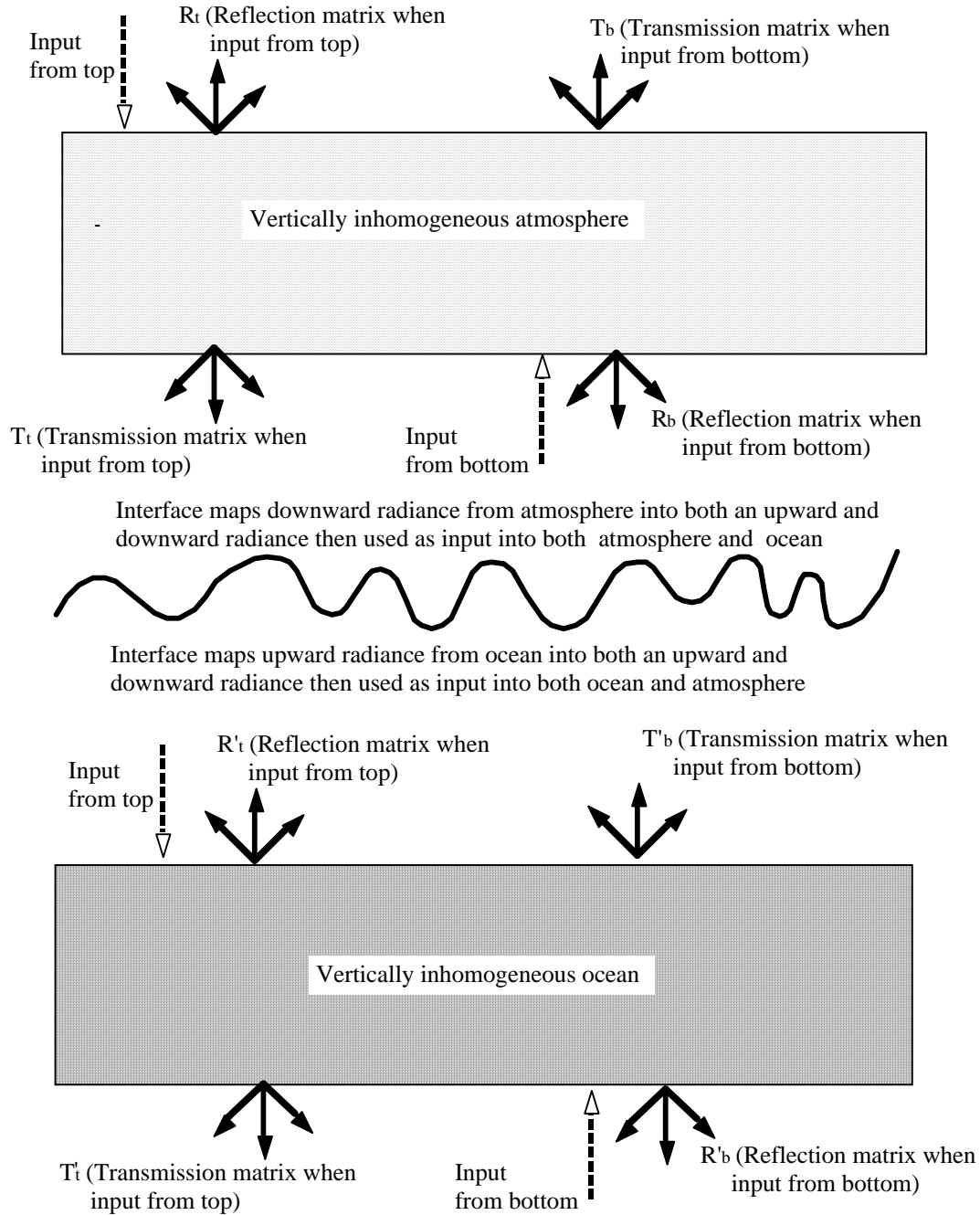


Figure 1. Schematic representation on the use of matrix operator theory to calculate the time dependent radiation field within the ocean

WORK COMPLETED

- a) We have developed a hybrid matrix operator – Monte Carlo (HMOMC) method to solve the vector radiative transfer equation (VRTE) in a 3D atmosphere-ocean system (AOS) . The primary advantage of this hybrid method is that it solves the VRTE efficiently in an AOS with different dielectric interfaces but with the same atmospheric and oceanic conditions. Two papers on this work have been submitted to Applied Optics.
- b) We have completed a study of the light scattering by a small volume element filled with randomly positioned particles and were able to include the variation of the particles' positions in the far-field modified uncorrelated single-scattering approximation (MUSSA) which leads to the incoherent summation of the phase matrices of particles in the volume. A paper on this work has appeared in Optics Express, 15, pp. 8479-8485 (2007).
- c) We have completed a study on the use of the finite-difference time-domain (FDTD) method to simulate the electromagnetic radiation emitted by an infinitesimal electric dipole embedded in a small particle with an arbitrary shape and internal composition. A paper on this work has appeared in JQSRT, 106, 257-261, (2007)
- d) We have completed a comparison of the volume-integral method (VIM) and the surface-integral method (SIM) by which the finite-difference time-domain (FDTD) technique transforms the near-field to the corresponding far-field when computing light scattering by a dielectric particle with large refractive indices. In this study, we show that the SIM allows a much coarser grid resolution than that required by the VIM. A paper on this work has appeared in JQSRT, 106, 590-594, (2007).
- e) We have completed a study of the use of short illuminating pulses in a cavity with highly reflecting walls and studying the temporal decay of the radiation in the cavity as a means to measure weak absorption in the cavity. A paper on this work has appeared in Applied Optics, 45, 9053-9065, (2006)
- f) We have completed a very thorough study of the asymptotic light field in the ocean where we have included polarization as well as Raman scattering. A paper on this work is presently being prepared for publication in Applied Optics.

RESULTS

- a). The HMOMC model is used to calculate the radiance field under a cosine ocean wave. The range of the computational domain is $-10.5 \text{ m} < x, y < 10.5 \text{ m}$ and $0 < z < 20 \text{ m}$. The ocean is within $0 < z < 10 \text{ m}$ and the atmosphere is within $10 \text{ m} < z < 20 \text{ m}$. The extinction coefficient of the atmosphere is 0.025 m^{-1} , which means the optical depth of the atmosphere is 0.25. The Rayleigh phase matrix is chosen for the atmosphere. The extinction coefficient of the ocean is 1.0 m^{-1} , making the optical depth of the ocean 10.0. The phase function P_{11} for the ocean is chosen as the Henyey-Greenstein (H-G) phase function. The asymmetry parameter $g=0.95$ is used for this case. The other phase matrix elements for the ocean are determined by letting the corresponding reduced phase matrix elements be equal to those of the reduced Rayleigh phase matrix elements. The single scattering albedo is 0.5 for the atmosphere, ocean, and the Lambertian ocean bottom. There are 81 grids in the x dimension, and there is only 1 grid in the y dimension. A cosine ocean wave is imposed between the atmosphere and the ocean, whose normal vectors are given by:

$$\begin{aligned}
n_x &= A \cdot \sin(2 \pi (K-1)/(N-1)), \\
n_y &= 0, \\
n_z &= 1, \\
\mathbf{n} &= (n_x, n_y, n_z) / \sqrt{n_x^2 + n_y^2 + n_z^2},
\end{aligned} \tag{1}$$

where the wave amplitude A is selected to be 0.3 m to make the maximum polar angle of the normal vectors less than 15° ; K is the index of the grids along the x dimension, which changes from 1 to N ; and $N=81$ is the maximum number of the grids along x . Figure 2 shows a sketch of the system. In Fig. 2, the four arrows at $K=1, 21, 41, 61$ shows illustrative wave normals at those locations. Four detectors are located below the locations depicted by the arrows. The four detectors are at the same horizontal level. The distance between the detectors and the dielectric interface is denoted by L_d , and the corresponding optical thickness is denoted by τ_d .

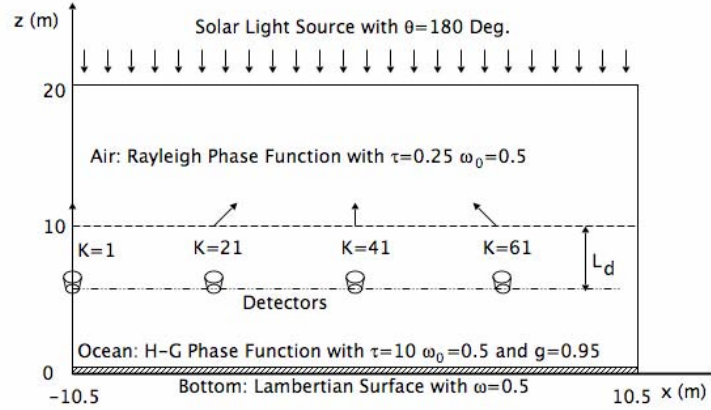


Figure 2. Schematic representation of a system of radiance under a cosine wave. The dashed line at $z=10$ m shows the position of the cosine wave. The four arrows at $K=1, 21, 41, 61$ show illustrative wave normals at those locations, where K is the index of the grids along the x dimension. Four detectors are located below the locations depicted by the arrows. The four detectors are at the same horizontal level. The distance between the detectors and the dielectric interface is denoted by L_d , and the corresponding optical thickness is denoted by τ_d .

The radiance field depends on the horizontal position of the detector. We calculated the radiance field distribution for the four detectors with three values of $L_d=0, 1, 5$, and the corresponding optical thicknesses $\tau_d=0, 1, 5$. Figure 3 shows the angular distribution of the downward radiance I at the four locations for $\tau_d=0$. The wave profile centered at each detector position are shown for all the panels in Fig. 3. Additionally, the normal vector of the wave at the detector position is also shown. In Fig. 3, the radiance distribution is transformed into a round disk image. For each pixel of the image, the magnitude of the radiance is shown by a color. A pixel at the center shows the radiance with a polar angle of 180° and a pixel at the outer edge shows the radiance with a polar angle of 90° . A pixel's azimuthal angle shows the corresponding azimuthal angle of the radiance. It is evident that the radiance distributions in Fig. 3 have two distinct regions. The radiance values in the inner region are greater than those of the outer region. The shape of the inner region is conical and centered at the normal vector of the ocean wave at that location. In the inner region, the radiance comes from both

directly transmitted light from the interface and multiple scattering, while in the outer region the radiance comes from multiple scattering only. This is the reason for the discontinuity between the two regions. The radiance distributions for $K=1$ and $K=41$ are azimuthally symmetric. This is because the normal vectors for these two cases are the same as those in the case of a flat interface. Furthermore, $\tau_d=0$ ensures there is no direct interaction between wave pixels with different K values.

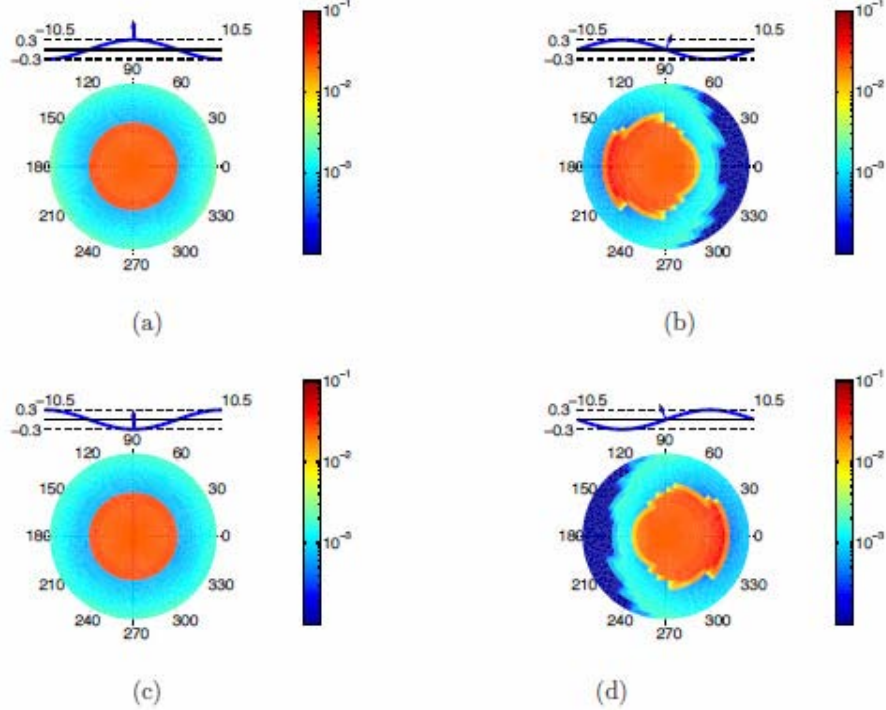


Figure 3. The angular distribution of the downward radiance I at four locations under a cosine ocean wave for a coupled atmosphere and ocean system shown in Fig. 2. $\tau_d=0.0$. (a) $K=1$, (b) $K=21$, (c) $K=41$, (d) $K=61$.

Figure 4 shows the radiance distribution under the cosine ocean wave for $\tau_d=1.0$. In Fig. 4, the radiance distribution still shows a bright inner region and a dark outer region. However, the boundary of the two regions is blurred. For $K=1$ and $K=41$, the radiance distributions are no longer azimuthally symmetric. This is due to contribution to the radiances coming from nearby wave pixels. The radiance distributions for $K=1$ and $K=41$ still conserve the symmetry along $\phi=0^\circ - 180^\circ$ and $\phi=90^\circ - 270^\circ$ planes. This is because the system is symmetric about these planes. The range of the bright region of $K=1$ has a smaller polar angle range along $\phi=0^\circ$ than that of the bright region along $\phi=90^\circ$. This is due to the focusing effect of the ocean wave maxima at $K=1$. On the contrary, the ocean wave minima at $K=41$ diverges the transmitted radiance. This is why the brightness region for $K=41$ shows the opposite feature. This observation can be used to detect maxima or minima for a one-dimensional ocean wave shown in our case. For a two-dimensional wave, one can tell the extent of the ocean wave along different dimensions based on the azimuthal pattern of the radiance distribution.

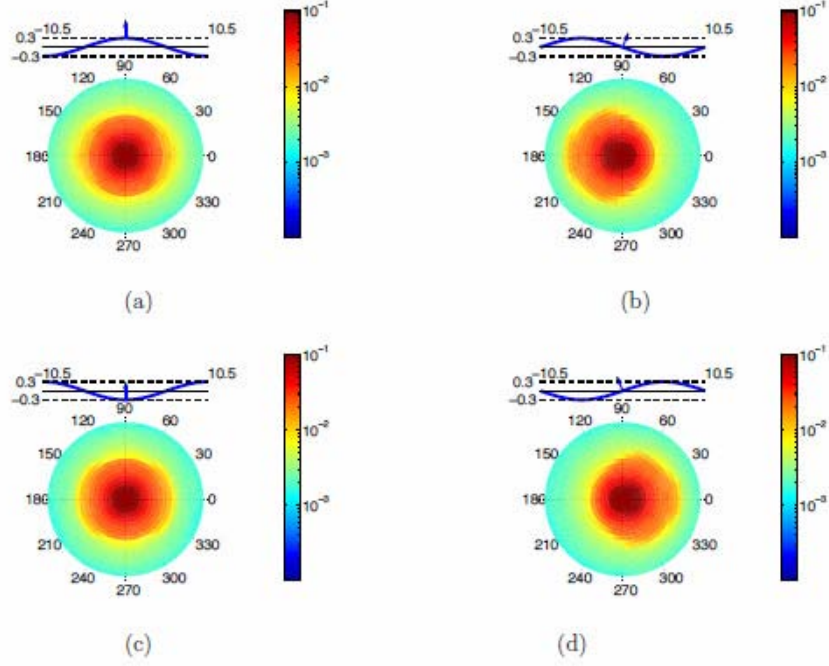


Figure 4. The angular distribution of the downward radiance I at four locations under a cosine ocean wave for a coupled atmosphere and ocean system shown in Fig. 2. $\tau_d = 1.0$. (a) $K=1$, (b) $K=21$, (c) $K=41$, (d) $K=61$.

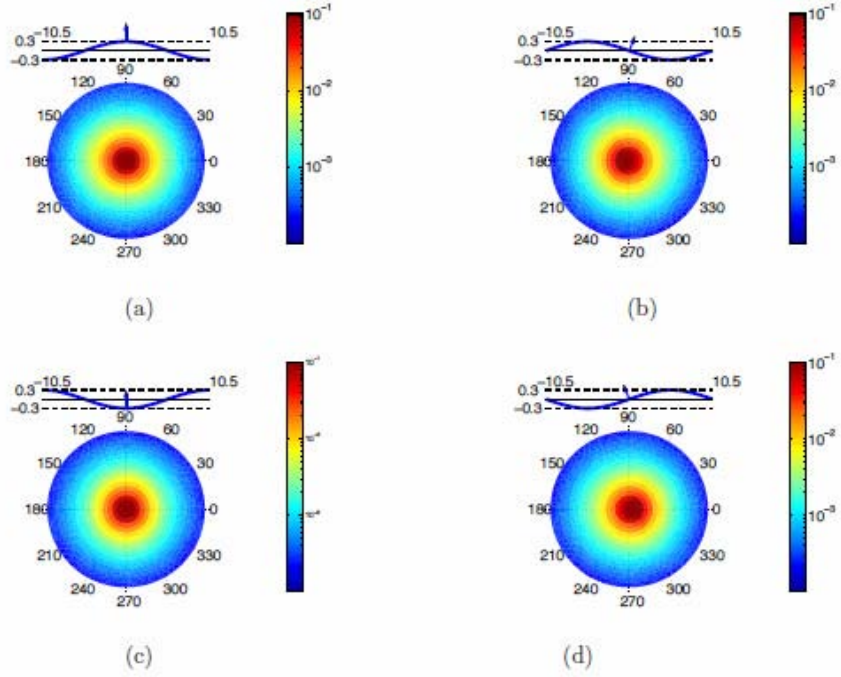


Figure 5. The angular distribution of the downward radiance I at four locations under a cosine ocean wave for a coupled atmosphere and ocean system shown in Fig. 2. $\tau_d = 5.0$. (a) $K=1$, (b) $K=21$, (c) $K=41$, (d) $K=61$.

Figure 5 shows the radiance distribution for the same system for $\tau_d = 5.0$. In Fig. 5, the boundary of the bright and dark regions are further blurred. Moreover, the variation of the radiance distribution becomes smaller as the detector moves along the x dimension, which is because the multiple scattering is more dominant for the large optical depth $\tau_d = 5.0$. At some point, the detectors will lose all information about the waves above them. The distribution becomes azimuthally symmetric regardless of the wave profile. This is called the asymptotic region of light scattering in the ocean

IMPACT/APPLICATION

This new code together with the previous 3D Monte Carlo code for solving the vector radiative transfer equation will become powerful tools to study the effects of a dynamic wave profile and 3D inhomogeneous hydrosol distribution on the radiance field. A further study based on our current code could lead to a fundamental development of underwater image detection and remote sensing of ocean color.

TRANSITIONS

Due to the efficiency and versatility of this new code, it will be directly applicable to understanding one of the most formidable problems in global warming, i.e. the effect of broken clouds on the reflectivity of the atmosphere. My colleague, Dr. Ping Yang in the Department of Atmospheric Sciences at TAMU, will use it to interpret the measurements for the new satellite Cloud-Aerosol Lidar and Infrared Pathfinder Satellite (CALIPSO).

RELATED PROJECTS

We use the results from our other ONR Grant to use as input to our codes in the RaDyO study

REFERENCES

1. G. W. Kattawar and G. N. Plass, "Asymptotic Radiance and Polarization in Optically Thick Media: Ocean and Clouds," *Appl. Opt.* 5, 3166-3178 (1976).
2. L. G. Stenholm, H. Störzer, and R. Wehrse, "An efficient method for the solution of 3-D Radiative Transfer Problems", *JQSRT.* 45. 47-56, (1991)
3. A. Sánchez, T.F. Smith, and W. F. Krajewski "A three-dimensional atmospheric radiative transfer model based on the discrete ordinates method", *Atmos. Res.* 33, 283-308, (1994)
4. J. L. Haferman, T. F. Smith, and W. F. Krajewski, "A Multi-dimensional Discrete Ordinates Method for Polarized Radiative Transfer, Part I: Validation for Randomly Oriented Axisymmetric Particles", *JQSRT*, 58379-398, (1997)
5. K.F. Evans, "The spherical Harmonics Discrete Ordinates Method for Three-Dimensional Atmospheric Radiative Transfer", *J. Atmos. Sci.*, 55, 429-446, (1998)
6. Q. Liu, C. Simmer, and E. Ruprecht, "Three-dimensional radiative transfer effects of clouds in the microwave spectral range", *J. Geophys. Res.* 101(D2), 4289-4298, (1996)

7. B. Mayer, "I3RC phase I results from the MYSTIC Monte Carlo model", Extended abstract for the I3RC workshop, Tucson Arizona, 1-6, November 17-19, (1999).
8. L. Roberti and C. Kummerow, "Monte Carlo calculations of polarized microwave radiation emerging from cloud structures", *J. Geophys. Res.* 104(D2), 2093-2104, (1999).
9. C. Davis, C. Emde, and R. Harwood, "A 3D Polarized Reversed Monte Carlo Radiative Transfer Model for mm and sub-mm Passive Remote Sensing in Cloudy Atmospheres", *Trans. Geophys. and Rem. Sens., Special MicroRad04 Issue*, (2004).
10. G. N. Plass, G. W. Kattawar and F. E. Catchings, "Matrix Operator Theory of Radiative Transfer I. Rayleigh Scattering," *Appl. Opt.* 12, 314-329 (1973).
11. G. W. Kattawar, G. N. Plass and F. E. Catchings, "Matrix Operator Theory of Radiative Transfer. II. Scattering from Maritime Haze," *Appl. Opt.* 12, 1071-1084 (1973).

PUBLICATIONS

1. P. Zhai, G. W. Kattawar, and P. Yang, "An Impulse Response Solution to the 3D Vector RTE in Atmosphere-Ocean Systems: Part II: The hybrid matrix operator - Monte Carlo method," submitted to *Applied Optics*, [in press, refereed].
2. P. Zhai, G. W. Kattawar, and P. Yang, "An Impulse Response Solution to the 3D Vector RTE in Atmosphere-Ocean Systems: Part I: The Monte Carlo Method," submitted to *Applied Optics*, [in press, refereed].
3. P. Zhai, G. W. Kattawar, and P. Yang, "The far-field modified uncorrelated single-scattering approximation in light scattering by a small volume element," *Optics Express*, Vol. 15, Issue 13, pp. 8479-8485, (2007). [published, refereed]
4. P. Zhai, C. Li, G. W. Kattawar and P. Yang, "FDTD Far-field scattering amplitudes: Comparison of surface and volume integration methods," *Journal of Quantitative Spectroscopy and Radiative Transfer*, Vol. 106 pp. 590-594, (2007). [published, refereed]
5. C. Li, G. W. Kattawar, Y. You, P. Zhai and P. Yang, "FDTD solutions for the distribution of radiation from dipoles embedded in dielectric particles", *JQSRT*, 106, 257-261, (2007) [published, refereed]
6. E.S. Fry, J. Musser, G.W. Kattawar, and P. Zhai, "Integrating Cavities: temporal response", *Applied Optics*, 45, 9053-9065, (2006). [published, refereed]